energies

MDPI

Article

Size-Segregated Particulate Matter from Gasification of Bulgarian Agro-Forest Biomass Residue

Ricardo Ferreira [1], Tsvetelina Petrova [2], Ana F. Ferreira [1,*], Mário Costa [1], Iliyana Inaydenova [2], Stela Atanasova-Vladimirova [3] and Bogdan Ranguelov [3]

[1] IDMEC, Mechanical Engineering Department, Instituto Superior Técnico, Universidade de Lisboa, 1049-001 Lisboa, Portugal; ricardo1995ferreira@gmail.com (R.F.); mcosta@tecnico.ulisboa.pt (M.C.)
[2] College of Energy and Electronics, Technical University of Sofia, 1000 Sofia, Bulgaria; tzvetelina.petrova@tu-sofia.bg (T.P.); inaydenova@tu-sofia.bg (I.I.)
[3] Institute of Physical Chemistry, Bulgarian Academy of Sciences, 1113 Sofia, Bulgaria; statanasova@ipc.bas.bg (S.A.-V.); rangelov@ipc.bas.bg (B.R.)
* Correspondence: filipa.ferreira@tecnico.ulisboa.pt; Tel.: +351-962447289

Abstract: The main purpose of the present work was to evaluate the efficiency of the gasification process of three different types of agro-forest biomass residue (rapeseed, softwood, and sunflower husks) along with the characterization of size-segregated particulates' emissions. The experiments were carried out in a drop tube furnace (DTF), using two different gasifying agents (O_2/N_2 and $O_2/N_2/CO_2$) at atmospheric pressure and a constant temperature of 1000 °C. In focus was the effect of biomass and the gasifying agent on syngas composition (CO, H_2, CH_4, and CO_2), cold gas and carbon conversion efficiency, and on the emissions of by-products, such as particulate matter (PM), known for having negative environmental and health impacts. The collected particulates were characterized by SEM/EDS and XPS analysis. The results reveal that: (i) the introduction of CO_2 increased the production of CO and CH_4 and syngas' lower heating value (LHV), thus leading to higher cold gas and carbon conversion efficiency; (ii) CO_2 decreased the production of H_2, leading to lower H_2/CO ratio (between 0.25 and 0.9). Therefore, the generated syngas is suitable for the synthesis of higher hydrocarbons, (iii) CO_2 lowered the emissions of char (cyclone) particles but increased the overall $PM_{10–0.3}$. Submicron size PM was the dominant fraction ($PM_{1–0.3}$) in O_2/N_2 and ($PM_{1.6–0.3}$) in $O_2/N_2/CO_2$. Unimodal PM size distribution was observed, except for sunflower husks gasification in $O_2/N_2/CO_2$; (iv) the SEM/EDS and XPS analysis confirmed that submicron-sized $PM_{1–0.3}$ contain above 80% of carbon associated to soot, due to incomplete oxidation, whereas in cyclone (char) particles, carbon decreased to about 50%. The SEM/EDS results showed that K and Cl are typical constituents of the submicron size PM, whereas the alkaline earth metals were detected mainly in fine and coarse particulates. Detailed analysis of the XPS (C1s) spectra showed that the most common oxygen-containing groups on the PM_1 surface were carbonyl and carboxyl.

Keywords: gasification; rapeseed; sunflower husk; softwood; particulate matter; syngas

Citation: Ferreira, R.; Petrova, T.; Ferreira, A.; Costa, M.; Inaydenova, I.; Atanasova-Vladimirova, S.; Ranguelov, B. Size-Segregated Particulate Matter from Gasification of Bulgarian Agro-Forest Biomass Residue. *Energies* **2021**, *14*, 385. https://doi.org/10.3390/en14020385

Received: 11 December 2020
Accepted: 6 January 2021
Published: 12 January 2021

1. Introduction

The recent energy demand, because of the growth of the Earth's population and intensive industry development, requires an energy supply at reasonable prices and availability. Combustion of fossil fuels has been and still is cost-effective and the world's primary source of energy. Thus, the influence of the secondary combustion products on the environment, climate, and the quality of life of humans and ecosystems is the focus of the recent research, along with the need for developing easy accessible alternative fuels (such as biomass) and low-emission utilization technologies. Most of the existing utilization technologies render significant social and economic pressure on society [1,2]. Most of the

contemporary technologies for utilization of conventional and/or alternative fuels, demand implementation of innovations, leading to improved energy-efficiency and reduced environmental impact. Currently, biomass appears as the fourth biggest energy source worldwide and under given circumstances it can be considered carbon-neutral, assuming that this fuel replaces the carbon dioxide (CO_2) that is captured [3–5]. Currently, the energy in Bulgaria is derived mainly from fossil fuel combustion [2]. In Bulgaria, there are 4 077 million hectares of forested lands, corresponding to 34% of the total territory. Thus, providing a significant annual amount of biomass that should be utilized in the most effective and environmentally friendly way [6].

The transformation of biomass to energy can be achieved through several processes. One of them is gasification, which is a thermo-chemical process, converting fossil or non-fossil fuels to solid, liquid, and gaseous products. Usually, a chemical reactor is used, operating at moderate to high temperatures, 700–1500 °C, [5] with the presence of a gasifying agent, e.g., oxygen, under sub-stoichiometric conditions. The resulting gas is called producer gas or synthetic gas (syngas) and it is mainly composed of carbon monoxide (CO), hydrogen (H_2), methane (CH_4), and a small amount of CO_2 and hydrocarbons. The syngas is flammable and combustible. It has a pronounced potential to be used for energy generation purposes, because it is relatively easy to clean, transport, and burn in a more efficient way, in comparison to the original feedstock [7]. The gasification process with coals as fuel is responsible for 30% of methanol and 25% of ammonia production worldwide [8]. Effective syngas cleaning is fundamental to have a clean engine operation [9]. According to the authors, the contaminants and heavy hydrocarbons are considered as tar or char that can be removed before the combustion process. They further discuss that tar removal still requires optimization, but char is a valuable product with a wide range of applications. The possible utilization concepts of the inert ash are also reviewed in [9], along with the syngas cleaning from fine PM through cyclones or water/oil scrubbers. However, some carbonaceous particles of different size and content, such as soot and char are freely released to the environment. The soot particles are of great concern as they are usually part of the submicron PM. Due to their small size and complex chemical composition, they specifically create problems for human health, since ultrafine particles can infiltrate in cardiovascular and respiratory systems, causing lung malfunction [10]. These PM are also known for creating problems downstream of the energy systems, such as equipment performance and durability [11], thus decreasing the carbon conversion efficiency [12]. Therefore, controlling the ultrafine particulates in the exhaust of such systems is a task of essential importance, requiring detailed research from experimental and theoretical points of view.

The gasification process can be affected by several key factors, the most important of which are as follows: fuel composition, gasifying atmosphere, operating pressure, temperature, moisture content of the fuels, the gasifiers' design, residence time, and heating rate [13–15]. The reactors that are typically used for gasification purposes include fixed or moving beds, fluidized beds (bubbling and/or circulating), entrained flow, and drop tube furnace (DTF). The use of entrained flow and a DTF is common in the study of biomass gasification under well-controlled conditions (temperature, residence time, fuel particle size, etc.). The gasifying medium (atmosphere) significantly influences the process. This can be composed of oxygen (O_2), air, CO_2, and steam, or a mixture of these compounds. The use of air leads to syngas with a low heating value due to the presence of nitrogen. The heating value of the syngas increases when pure oxygen is used. However, in such cases, an air separation unit is required, which makes the process more expensive. If steam is used in the gasifying medium the water-gas shift reaction is promoted, generating a high percentage of hydrogen, while the tars yield is decreased due to the decomposition of the organic pyrolytic vapors [4,13]. Finally, when CO_2 is added as a gasifying agent, the formation of CO increases while the formation of char is decreased. The negative effect, in this case, is the reduced production of H_2 and the LHV of the obtained syngas [16].

The agro-forest biomass residue is an adequate feedstock for gasification purposes. Rapeseed residue has gained significant interest, since the stalks of rapeseed are widely available, mainly for bio-oil production. Gao et al. [17] investigated the impact of the temperature on products' (solid charcoal, liquid oil, and gaseous products) characteristics obtained during rapeseed stalk pyrolysis. The tests were conducted in a fixed-bed reactor at a temperature between 250 and 950 °C. The results disclose that at temperatures above 550 °C, the liquid oil and solid char yield decreases, while the combustible gas products (H_2, CH_4, CO, CO_2, C_2H_4, C_2H_6, and C_2H_2) yield increases. Burhenne et al. [18] studied pyrolysis of three types of biomass (rape straw, wheat straw, and spruce wood) in a fixed bed reactor. The biomass was heated at a slow heating rate of 20 K/min up to 773 K. The results pointed out that the CO_2 volume in the product gas was almost twice that of the CO volume for the two straw types. The CH_4 yield did not differ significantly among studied samples. The lowest portion in the product gas was for H_2. The two types of straw showed a higher H_2 fraction compared to the wood biomass. Sattar et al. [19] gasified rapeseed, wood, sewage sludge, and miscanthus biochar at intermediate temperatures (700–750 °C). The authors obtained a high concentration of H_2 together with high mineral composition in the yielded char.

Softwood is another type of biomass suitable for gasification [20–23]. Mandl et al. [20] gasified softwood pellets in an updraft fixed-bed gasifier. The main results showed a considerable impact of the airflow rate on the composition of the producer gas, while the increase of the airflow resulted in increasing of CO, due to the improved char gasification. Aghaalikhani et al. [21] carried out detailed modeling of softwood pellets in a dual fluidized bed gasifier with steam The simulations corresponded well with the experimentally measured parameter and showed that increasing the temperature leads to higher H_2 and CO in the resulting gas, while the yield of CO_2 and CH_4 decreased. Tsalidis et al. [22] studied the effect of torrefaction on the gasification behavior of softwood (spruce) and hardwood (ash). For this purpose, a steam-oxygen blown circulating fluidized bed gasifier was used. The authors' observation was that the torrefaction resulted in a limited impact on the constituents of the product gas, but the cold gas efficiency and the carbon conversion efficiency decreased significantly. The conclusion was that the torrefaction of both softwood and hardwood was not recommended in the gasification process. Mauerhofer et al. [23] investigated the impact of CO_2 in the gasification atmosphere on the main product gas component during softwood gasification in a dual fluidized bed reactor. The experiments were performed with a mixture of CO_2 and steam in different proportions. The authors reported that increasing the CO_2 portion in the gasifying mixture decreased the yield of H_2 and CH_4, while the presence of CO and CO_2 grew in the product gas composition.

According to the Bulgarian Ministry of Agriculture, Food and Forestry [24], the average annual production (2016–2020) of rapeseed and sunflower is 406,707 t and 1,756,483 t, respectively. There are studies, focused on the gasification of sunflower husk [25–27], but it is hard to find detailed investigations on sunflower husk gasification in conditions typical for a DTF. Cabuk et al. [25] examined the impact of biomass torrefaction on the H_2 production during gasification of torrefied biomass and its blend with lignite. For this purpose, sunflower seed cake was torrefied at 250, 300, and 350 °C. The authors concluded that the torrefied sunflower seed cake, instead of the raw one, is a promising feedstock for H_2 production through steam co-gasification with lignite in both fluidized bed and downstream reactors, after some alteration. Mojaver et al. [27] model biomass gasification in fluidized bed conditions in a steam atmosphere. The model was verified with experimentally obtained results. The work considered 13 different types of biomass, including sunflower husks. The authors concluded that hydrogen production increased by increasing the steam quantity and temperature, while the CO_2 syngas concentration decreased at a lower steam quantity and higher temperature for all studied biomass types.

Recently in Bulgaria, the atmospheric PM was characterized with a general focus on PM_{10} and $PM_{2.5}$. The PM investigations were carried out mainly in two directions, as follows: (a) monitoring the concentration of PM_{10} and $PM_{2.5}$ in the atmospheric air and its dispersion [28–31] by experimental techniques or computational models; (b) characterization of atmospheric PM in terms of their chemical composition [32–34]. A lack of detailed characterization of the PM emitted during typically applied utilization processes of locally produced and provided blends of biofuels was observed. Moreover, such solid biofuels are typically used in small- and medium-scale energy systems providing household heating services. Thus systematic research is needed concerning the PM of a wide range of sizes ($PM_{10–0.1}$) that can be obtained directly from the flue gases. Once exhausted in the atmosphere, these particulates undergo numerous chemical transformations. Therefore, of significant importance is the PM characterization with regard to their chemical composition, structure, size distribution, etc.

The global objective of the present work was to evaluate the efficiency of the gasification of three different types of agro-forest biomass residue as well as to study the effect of biomass and gasifying agent on the syngas production, and its composition, along with the emissions of harmful by-products, size-segregated PM, formed during gasification of rapeseed, softwood, and sunflower husks in DTF. The experiments were performed at a fixed temperature of 1000 °C (conditions stimulating soot formation), and the reported data quantified the influence of CO_2 on the carbon conversion and the cold gas efficiency. The morphology and the elemental composition of the obtained particulates were characterized through SEM/EDS and XPS analysis.

The present study is one of a series of investigations, focused on the conversion of lignocellulosic biomass residue that is used for solid biofuel production and such fuels are already available at the Bulgarian market. The study is highly motivated by the currently observed interest in the country on biomass usage for power production [35]. Such an initiative requires detailed research on the locally obtainable blends of biomass fuels, involving different conversion techniques. The regular reports of the Member State show municipalities with exceedance of PM, in the context of the European legislation [36], according to which about 50% of the PM_{10} and above 80% of the $PM_{2.5}$ are due to household heating [37]. Herein only some preliminary results are presented relevant to biomass gasification in a DTF.

2. Materials and Methods

In the present work, three types of biomass residue (in the form of pellets), freely available on the Bulgarian energy market, were investigated: rapeseeds (RP), softwood (SW), and sunflower husks (SFH). Their chemical characteristics are presented elsewhere [38], but a summary is given in Table 1. Prior to the experiment, the biomass was crushed and sieved (using a mechanical sieve shaker with 250 μm sieve mesh) to sizes between 200 and 250 μm. To remove the moisture, all three biomasses were dried in an oven at 100 °C to 105 °C before each test.

Table 1. Chemical characteristics of the used biomass, as reported elsewhere [38].

Parameter Studied	SW	SFH	RP	Parameter Studied	SW	SFH	RP
Proximate analyses (wt. %, as analyzed)				Ash analysis (wt. %, dry basis)—normalized			
Moisture	6.89	7.52	9.86	SiO_2	3.60	1.44	3.32
Ash	0.65	2.88	4.59	Al_2O_3	7.05	0.21	1.31
Volatile organic compounds (VOC)	78.77	76.93	78.53	Fe_2O_3	2.26	1.31	0.34
Fixed carbon (by dif.)	13.69	12.67	4.59	MnO	2.10	0.03	0.08
Ultimate analysis (wt. %, as analyzed)				CaO	43.71	29.18	39.13
Carbon	47.77	54.04	49.64	MgO	9.77	17.06	12.60
Hydrogen	6.48	8.45	8.24	BaO	0.24	0.01	0.07
Nitrogen	0.14	3	2.67	Na_2O	1.29	0.81	3.34

Sulfur	<0.02	<0.05	<0.05	K_2O	20.69	41.08	23.96
Chlorine	na	<0.10	<0.10	Cr_2O_3	0.01	0.10	0.01
Oxygen (by dif.)	38.05	23.96	24.85	TiO_2	0.42	0.20	0.11
Higher heating value, (MJ/kg, dry basis)				ZnO	1.22	0.09	0.01
HHV	20.28	20.28	18.69	CuO	0.04	0.04	0.01
				SrO	0.01	0.03	0.03
				P_2O_5	7.59	8.39	15.71

Figure 1 visualizes the experimental setup used in the present study. The experimental installation consisted of biomass feeder, gas supply system, laboratory-scale DTF, particle sampling system, gas sampling, and gas analyzing systems. The feeder, positioned on the top of the DTF, dosed the needed amount of the pulverized biomass which was conveyed with gas to the DTF's gasification chamber. In this experiment, N_2 was used. The DTF is an electrically heated ceramic tube with an inner diameter of 40 mm and a length of 1.75 m. The DTF temperature was constantly controlled by three thermocouples of type-K. The gases that compose the gasifying agent stream were all supplied from pressurized bottles.

The particle collection system consisted of two cyclone filters and a low pressure 13-stage cascade impactor (DLPI, Dekati® Ltd., Kangasala, Finland). The cyclone filters were an in-house made cyclone, which caught the particles with an aerodynamic diameter above 10 μm, and a commercial Dekati® cyclone that guaranteed the collection of particles with a 50% efficiency cut off at 10 μm. The 13-stage impactor captured particles with sizes between 10 μm and 0.030 μm. The remaining particles were collected in the low-pressure impactor. The particle collection system was kept at temperatures above 150 °C using heat blankets against gas condensation during the tests. Before and after each test run, the filters were weighted to determine the mass of the sampled PM.

The composition of the gaseous products was experimentally measured, using the following equipment: paramagnetic pressure analyzer for measuring the excess of O_2; non-dispersive infrared analyzer (for CO_2 and CO); gas chromatograph (GC) of type Clarus 500 was used for analyzing the concentration of H_2, CH_4, and some light hydrocarbons in the generated syngas.

The experiments, subject to the present study, were carried out at a DTF wall temperature of 1000 °C. The present study puts an accent on the emissions of secondary by-products, having harmful environmental and health effects. The choice of the gasification temperature was based on preliminary studies of biomass gasification, using similar equipment [24]. The authors observed that under the chosen conditions the highest soot yield could be obtained, which was expected to highly influence the emissions of fine particulates in the flue gases.

The effect of biomass type and two different gasifying agents were studied. The first one consisted of 1% of O_2 and 99% of N_2, while the other one was a mixture of 1% O_2, 93.5% N_2, and 5.5% CO_2. The biomass feed rate was around 15 g/h. The oxygen equivalence ratio, λ (the ratio between the oxygen fed and the stoichiometric oxygen needed for the biomass oxidation) was 0.4. The residence time of the fuel particle in the reactor was between 2.0 and 3.0 s. The total inlet of the gas flow was 10 dm^3/min, using N_2 to reach it.

According to Villeta et al. [9], different parameters can be used to evaluate the conversion rate of a biomass gasifier. At present, three parameters were used to assess the efficiency of the gasification process, namely the cold gas efficiency (CGE), the carbon conversion efficiency (CCE), and the ratio of H_2/CO.

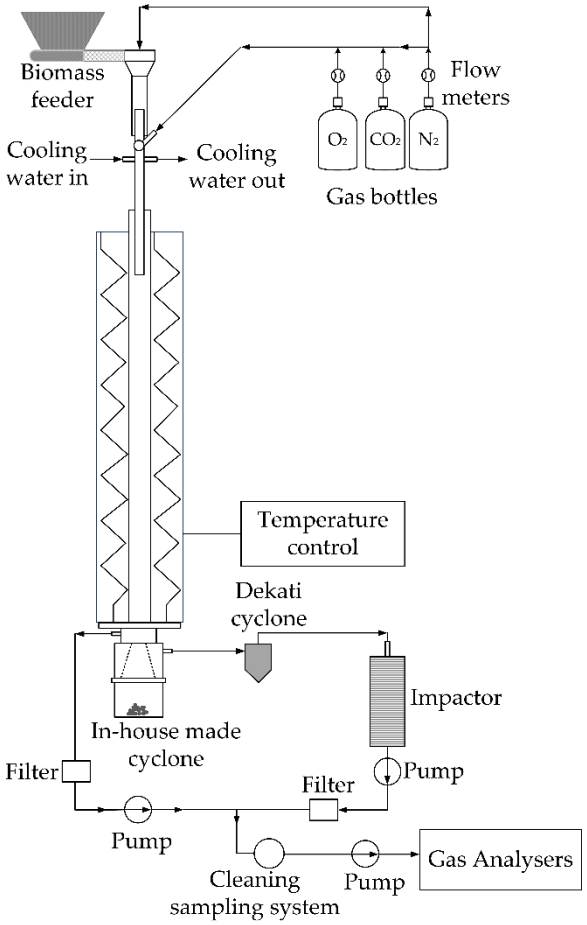

Figure 1. Scheme of the experimental installation.

Thus, the CGE is the ratio between the chemical energy leaving the reactor in the syngas form and the chemical energy entering the reactor with the biomass [9,39,40]. It can be estimated by the following equation:

$$\mathrm{CGE} = \frac{Q_{\mathrm{syngas}} \cdot LHV_{\mathrm{syngas}}}{\dot{m}_{\mathrm{bio}} \cdot LHV_{\mathrm{bio}}} \quad (1)$$

where LHV_{syngas} and LHV_{bio} are the lower heating values of the produced syngas and the initial biomass, respectively.

The CCE is normally determined through the ratio between the carbon leaving the gasifier as syngas (in the form of CO, CO_2, etc.) and the carbon entering the gasifier [9,39,40]. Thus, the following equation can be applied:

$$\mathrm{CCE} = \frac{Q_{\mathrm{syngas}} \cdot \sum_i^n x_{\mathrm{carbon,i}}}{\dot{m}_{\mathrm{bio}} \cdot y_{\mathrm{carbon}}} \quad (2)$$

where Q_{syngas} is the syngas flow rate (in Nm^3/h); x_{carbon} is the molar fraction of carbon in the products; $\dot{m}_{\mathrm{bio}}$ is the feeding mass rate of the biomass (in kg/h), and y_{carbon} is the carbon mass fraction from the ultimate analysis of the biomass. In the present experiment, the CCE was calculated through Equation (2). However, when $O_2/N_2/CO_2$ was used as the gasifying agent, only the CO_2, produced during the gasification process was considered.

The morphology and elemental composition of the sampled particulates were detected by the SEM-EDS technique using JEOL JSM 6390 apparatus, equipped with an INCA Oxford EDS detector.

In addition, X-ray photoelectron spectroscopy (XPS) studies were performed to obtain the primary elemental composition and the functional groups, available on the parti-

cle surface. For that purpose, a VG Escalab II system was implemented, using AlKα radiation with an energy of 1486.6 eV. The chamber pressure was 1.10–9 Pa. The Al_2p and Si_2p lines at 72.7 eV and 103.5 eV respectively were applied as an internal standard in the calibration procedure, with regard to the binding energies (BE). The corrections in the photoelectron spectra were based on the subtraction of the Shirley-type background. Their quantities were determined through the peak area and the Scofield's photo-ionization cross-section. The measured BE was obtained with an accuracy of ±0.2 eV.

3. Results

3.1. Gaseous Products—Syngas

The primary syngas compounds obtained during biomass gasification were: CO, CO_2, CH_4, and H_2. The effect of biomass type and the choice of the gasifying agent in the syngas composition is presented in Figure 2. Similar trends were observed for all gasified biomass types. Generally, the production of CO and CH_4 showed a slight increase in the presence of CO_2 in the reaction atmosphere, whereas H_2 and CH_4 concentrations slightly decreased. This effect was least expressed during softwood gasification.

As expected, CO_2 concentration in the exhaust decreased, when $O_2/N_2/CO_2$ was used as the gasifying agent, because it reacts with the formed char [16]. The results are in accordance with the observations of Mauerhofer et al. [23], who reported that the introduction of CO_2 in the gasification atmosphere of pellets made of softwood increases the CO yield. Shen et al. [41] reported syngas production during gasification of woody pellets in a fixed bed reactor. The authors compared the effect of two different gasifying agents: air and air/CO_2 on syngas production. When solely air is used, higher H_2 and CO concentrations are reported. However, the gasification temperature at the experiment, reported in [41], is below 1000 °C.

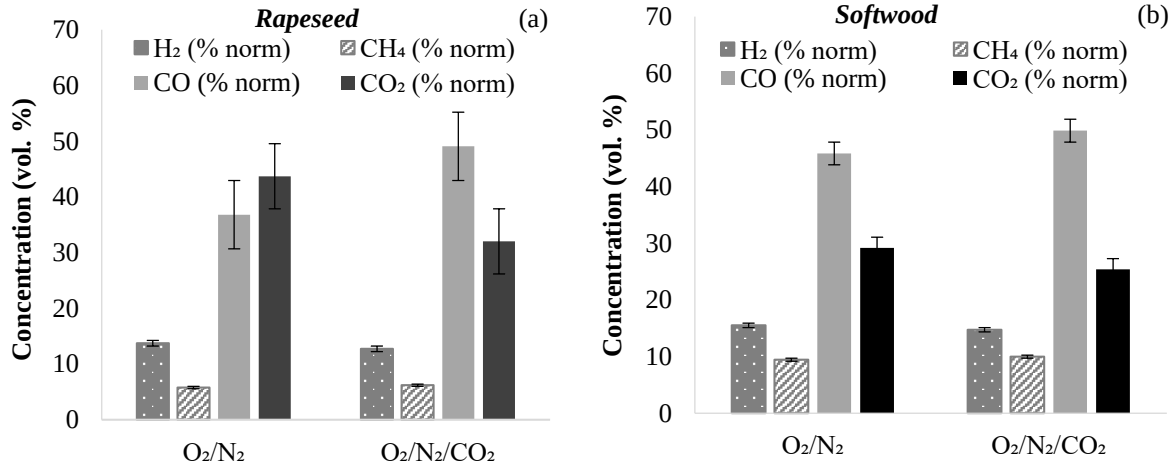

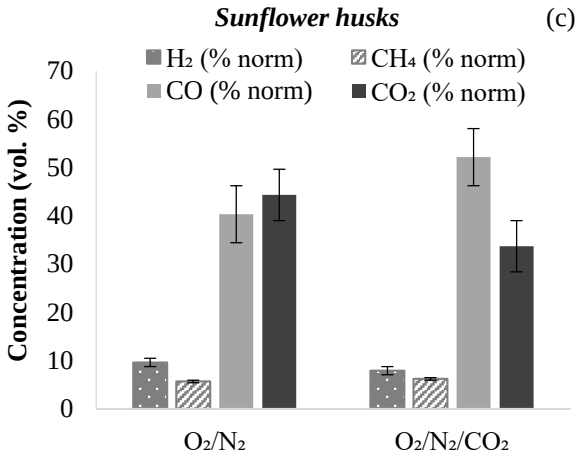

Figure 2. Effect of biomass and gasifying agent on syngas composition during gasification of (**a**) rapeseed, (**b**) softwood, and (**c**) sunflower husks in a drop tube furnace (DTF), at 1000 °C.

The CGE obtained in the present experiment, for all three biomass types, is presented in Figure 3 (left). Gasification of agriculture residue led to about 20% lower CGE in O_2/N_2 atmosphere (48.62% for the sunflower husks and 53.01% for the rapeseed). The CGE considerably increased when CO_2 was added to the gasifying mixture (65.56% for the sunflower husks and 70.65% for the rapeseed). There was a lesser effect of the gasifying agent on the CGE in softwood gasification (70.21% in O_2/N_2 and 74.80 in $O_2/N_2/CO_2$), and the maximum CGE was also obtained during softwood gasification in $O_2/N_2/CO_2$.

The results are in line with other studies. Pohořelý et al. [16] observed similar tendencies in wood chips gasification. The authors compared the use of different gasification atmospheres: $CO_2/O_2/N_2$, H_2O/O_2, and N_2/O_2 in a catalytic fluidized bed of dolomitic limestone. They reported that the CGE obtained when CO_2 is introduced in the gasification atmosphere was higher than when solely O_2 and N_2 were used. Furthermore, they stated that the use of CO_2 increased the carbon and energy conversion efficiency and decreased the quantity of tar in the produced gas. However, the CGE obtained in their work was close to 100%, since the authors used a different type of reactor.

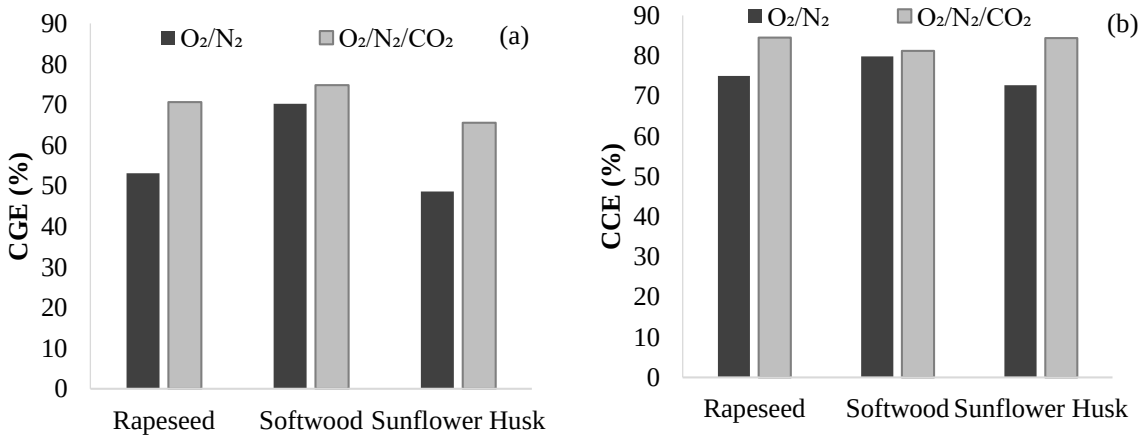

Figure 3. Effect of biomass and gasifying agent on (**a**) calculated cold gas efficiency (CGE) and (**b**) carbon conversion efficiency (CCE).

Duarte [39] reported that the CGE obtained during biomass gasification in a DTF typically varied between 55 and 90%. The author studied wheat straw gasification in a DTF at 1000 °C and reported CCE = 66.15%, CGE = 37.49%, and H_2/CO = 0.3. Billaud et al.

[13] described (also reported by Duarte [39]) the effect of additives, such as steam, CO_2, and O_2 on the CGE, carbon conversion, and formation of tar and soot during gasification of beech wood in a DTF. The experiment was performed in a relatively wide range of temperatures (between 800–1400 °C) and air equivalence ratios (ʎ, between 0.24 and 0.61). The authors concluded that the CGE increased with increasing ʎ and T up to 1200 °C, but it was found to decrease at the higher temperatures (up to 1400 °C).

Waldheim and Nilsson [42] studied the heating values of gases formed during biomass gasification and reported an increase of CO production when a gasification atmosphere containing CO_2 was used. The effect was attributed to the increased overall LHV of the syngas, which leads to an increase of CGE (Equation (1)).

The efficiency of carbon conversion (Figure 3 (right)) was similar to the CGE trend, since the increase of CO and CH_4 was bigger than the decrease of CO_2, as observed in Figure 2. The maximum increase of the CCE was found during the gasification of rapeseed in $O_2/N_2/CO_2$. Adánez-Rubio et al. [43] gasified pig manure in a similar experimental setup, using $O_2/N_2/CO_2$ and O_2/N_2 atmospheres. The experiments were carried out between 900 and 1200 °C, including the temperature used in this work, 1000 °C. The results showed that the addition of CO_2 to the gasifying agent (O_2/N_2) increased the CCE, due to the increase of CO mainly, and to the increase of CH_4.

Tsalidis et al. [22] investigated the impact of torrefaction on the performance characteristics of oxygen-steam blown circulating fluidized bed gasification of woody biomass (hardwood and softwood) and reported CCE = 89.1%; CGE = 53.4% and H_2/CO = 2.3.

The H_2/CO ratio and LHV of the syngas obtained in the present experiment are shown in Figure 4. This parameter (H_2/CO) is often used for estimating the possible application of the generated syngas, e.g., whether it is suitable to be used for energy production, further processing through Fischer-Tropsch reaction, or to produce long-chain hydrocarbons [44].

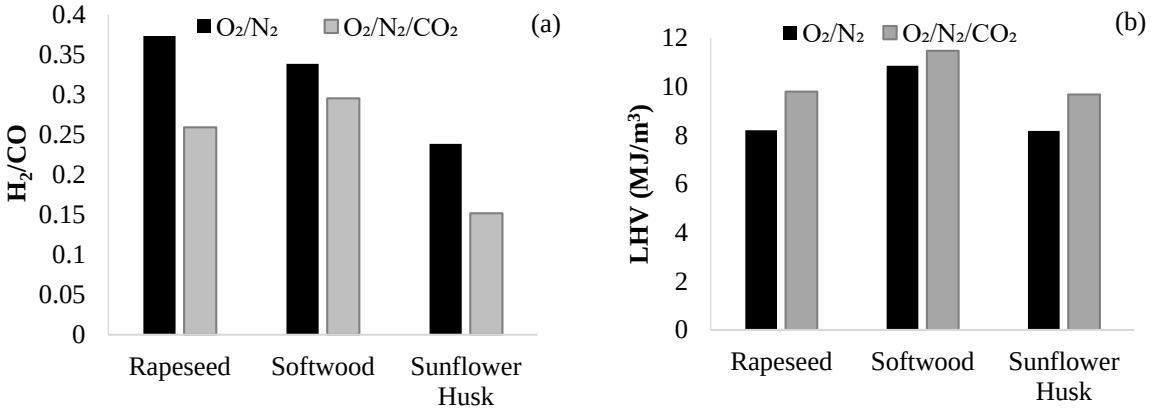

Figure 4. Effect of biomass and gasifying agent on (**a**) H_2/CO ratio and (**b**) LHV.

The H_2/CO ratio obtained in the present experiment reduced with introducing CO_2 in the gasification atmosphere, due to the decreased H_2 and the increased CO concentration. The highest obtained H_2/CO ratio (0.37) was during rapeseed gasification with O_2/N_2. Thus, the syngas generated in the present work cannot be directly used in a Fischer-Tropsch process, since it requires H_2/CO ratios between 2 and 3 [25–27]. The produced syngas can be processed for the synthesis of long-chain hydrocarbons, where the required H_2/CO ratios are much lower (between 0.25 and 0.9), and CO_2 is also needed. In a similar experiment, Adánez-Rubio et al. [43] reported H_2/CO ratios within the same range. The LHV, determined by the same authors, was in line with the present observations, according to which the LHV increased when $O_2/N_2/CO_2$ was used as a gasifying atmosphere. Currently, the effect was independent of the biomass type.

3.2. Solid Particles

The present work was focused on particulates, sampled using the equipment, described in Section 2. Both cyclones collected particulates with an aerodynamic diameter larger than 10 μm, which further in the text for simplicity are named cyclone particles. The low-pressure 13-stage cascade impactor collected only fine particulates of type PM_{10} to $PM_{0.3}$. Table 2 shows the relative mass of the cyclone particles and the total PM (mg) generated per biomass (g), expressed in dry basis (db) in both gasification atmospheres.

Table 2. Effect of the gasifying atmosphere on the mass of particles, sampled with both cyclones and with the 13-stage impactor (PM-13).

Biomass	RP (mg/g, db)		SFH (mg/g, db)		SW (mg/g, db)	
Gasifying Gas	O_2/N_2	$O_2/CO_2/N_2$	O_2/N_2	$O_2/CO_2/N_2$	O_2/N_2	$O_2/CO_2/N_2$
Cyclone	139.30	85.24	146.04	69.65	110.6	76.56
PM-13	2.228	7.268	6.992	9.972	6.528	7.206

The highest mass of cyclone particles was obtained during biomass gasification in O_2/N_2, whereas the overall mass of PM, caught in the impactor, was lower. The gasification of rapeseeds showed the lowest concentration of PM of a size below 10 μm in O_2/N_2 atmosphere (2.23 mg/g of biomass, db).

The total mass of the cyclone particles was considerably reduced during biomass gasification in $O_2/N_2/CO_2$. The highest decrease was obtained for the sunflower husk: from 146.04 mg/g of biomass, db (for O_2/N_2) to 69.65 mg/g of biomass, db (for $O_2/N_2/CO_2$).

Figure 5 discloses the effect of biomass and gasifying agent on PM mass and size distribution. The particulates, collected in filters 5–8 (i.e., $PM_{0.3}$, $PM_{0.4}$, $PM_{0.65}$, and PM_1) had the main contribution to the total PM mass. Rapeseed (a) had the lowest PM mass regarding both gasifying agents. Biomass gasification in $O_2/N_2/CO_2$ increased the PM emissions (about 2.5 times for rapeseeds, 1.8 times for softwood, and 2.2 times for sunflower husks), due to the enhanced rate of carbon conversion.

According to [45], during biomass combustion, the submicron-sized particles often show the highest number density, but they do not conduce considerably to the total mass of the PM. However, in the present experiment, the submicron particulates contributed significantly to the total mass of PM, collected with the low-pressure impactor, regardless of the gasification atmosphere. The total mass of the submicron PM, derived from the sum of the PM mass, obtained from filters 5 and 8 ($PM_{0.3}$, $PM_{0.4}$, $PM_{0.65}$, and PM_1), in O_2/N_2 was as follows: 84.56 wt % (rapeseed); 94.24 wt % (sunflower husk); 78.95 wt % (softwood), whereas in $O_2/N_2/CO_2$ it was: 91.53 wt % (rapeseed); 79.16 wt % (sunflower husk); 57.00 wt % (softwood). Similar results were reported in previous studies [38,46]. Gao and Wu obtained in situ volatiles during fast pyrolysis of wood at 800–1000 °C and combusted them in a DTF at 1300 °C. The authors investigated the contribution of volatiles to the emissions of submicron particulates (PM_1). Thus, the main part of Na, K, and Cl (43.5–97.2%) was volatilized and the sequential combustion of Na-, K-, and Cl-containing volatiles conduced greatly to PM_1 (77.4–89.3% of total PM_1 sampled during the combustion of volatiles and char). Naydenova et al. [38] observed that PM emission is highly influenced by the presence of both volatile matter and ash compounds. Submicron size PM (between 0.1 and 2.5 μm, with maximum concentration for the particulates of size around 0.25 μm) showing unimodal size distribution, were the prevailing portion in the combustion of five different biomass types in a bubbling fluidized bed reactor (700–900 °C). In addition, the PM number density was about three orders of magnitude lower during char combustion and shifted towards smaller PM (between 0.1 and 1 μm), with a maximum of around 0.2 μm.

Unimodal PM distribution was obtained for all three biomass types, gasified in O_2/N_2. Peaks of the relative mass of PM were obtained between filters 5 and 8 (at PM below 1 μm: 0.4 μm in rapeseed; 0.6 μm in softwood and sunflower husks). However, biomass

conversion in the presence of CO_2 led to a slight peak shift to the right (peaked at 1 µm in rapeseed and sunflower husk and at 1.6 µm in softwood (filter 9)). The effect of CO_2 in softwood resulted in a bimodal PM distribution, designated in the range between 0.3 and 1.6 µm (filters 5 to 9).

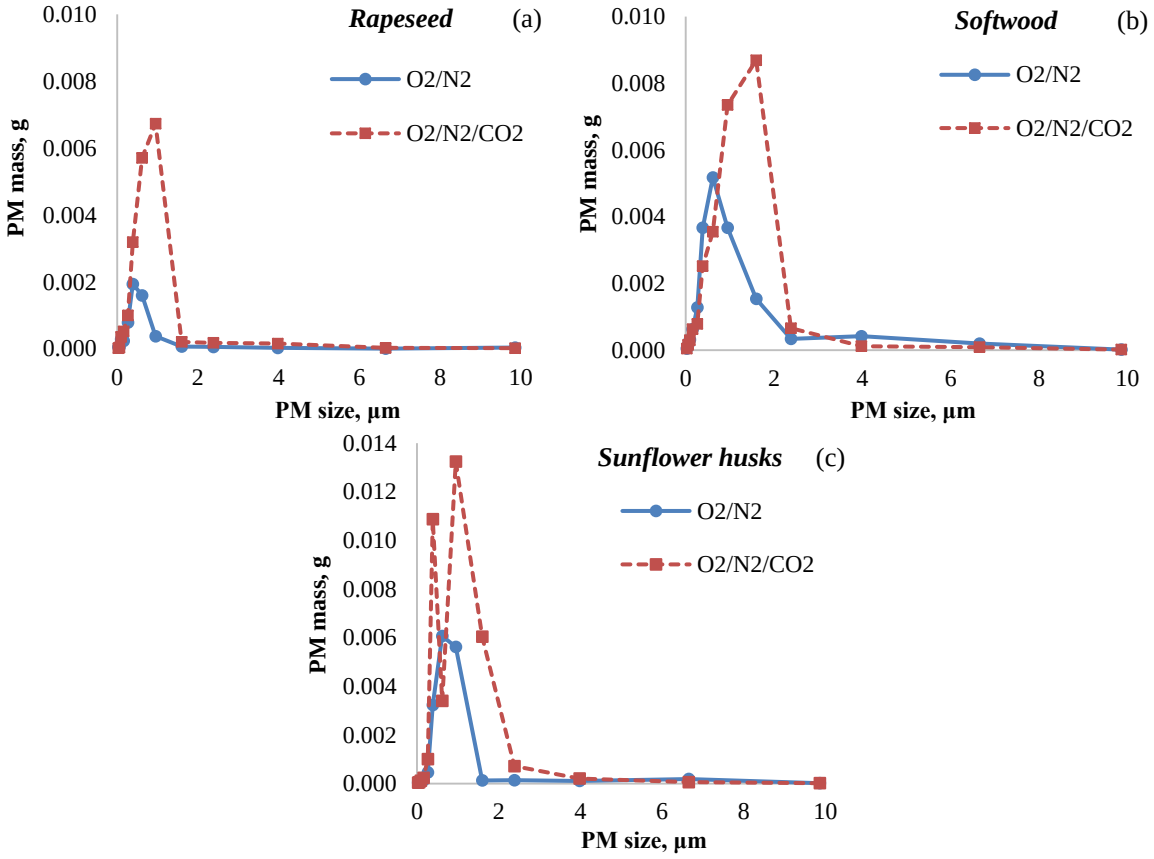

Figure 5. Effect of the gasifying agent on PM size and mass distribution for the different biomass (**a**) rapeseed, (**b**) softwood, and (**c**) sunflower husks.

Hermansson et al. [47] investigated PM size distribution during wood chips gasification in a direct fluidized bed gasifier. The authors used a similar low-pressure PM impactor and two PM maximums: one in the range of 0.1 to 0.6 µm and the other between 5–7 µm. In line with the present observations, the reported in [47] general results showed the highest measured number density of submicron PM at approximately 0.3 µm.

Chen et al. [48] reported bimodal PM size distribution in lignite and anthracite coal combustion, in the range of PM size between 0.1 and 1 µm. The authors attributed the emissions of submicron PM mainly to the process of vaporization, condensation, and nucleation of particular ash-forming inorganic compounds.

In contrast to biomass combustion, the present experiment was carried out in a low oxygen atmosphere (λ = 0.4). As expected, the major constituents of the submicron PM were carbon-containing particles (e.g., soot). This conclusion was confirmed through the SEM/EDS and the XPS analysis of these PM.

In the present study, SEM-EDS analysis was applied to the PM sampled on filters 8 (PM_1), and the effect of biomass and the gasifying agent was investigated. The EDS results indicated a significant amount of carbon among all filter 8 samples (PM_1). In an atmosphere of O_2/N_2, the PM_1 showed 88.08% of carbon for rapeseed, 88.86% for softwood, and 91.88% for sunflower husks. In the case of $O_2/N_2/CO_2$, the PM_1 carbon content was between 90.23% (rapeseed) and 94.63% (softwood).

Figure 6 shows the SEM images of PM from all filter 8 (PM_1). A particular accent was put on the PM_1 and smaller particulates. Although they are not yet regularly monitored

by European legislation, this type of particle is known for having significant environmental and health impacts. According to [39], the submicron-sized PM obtained during biomass gasification contains a significant amount of carbon (above 80%), usually reported as soot, because of the incomplete oxidation of the fuels' hydrocarbons.

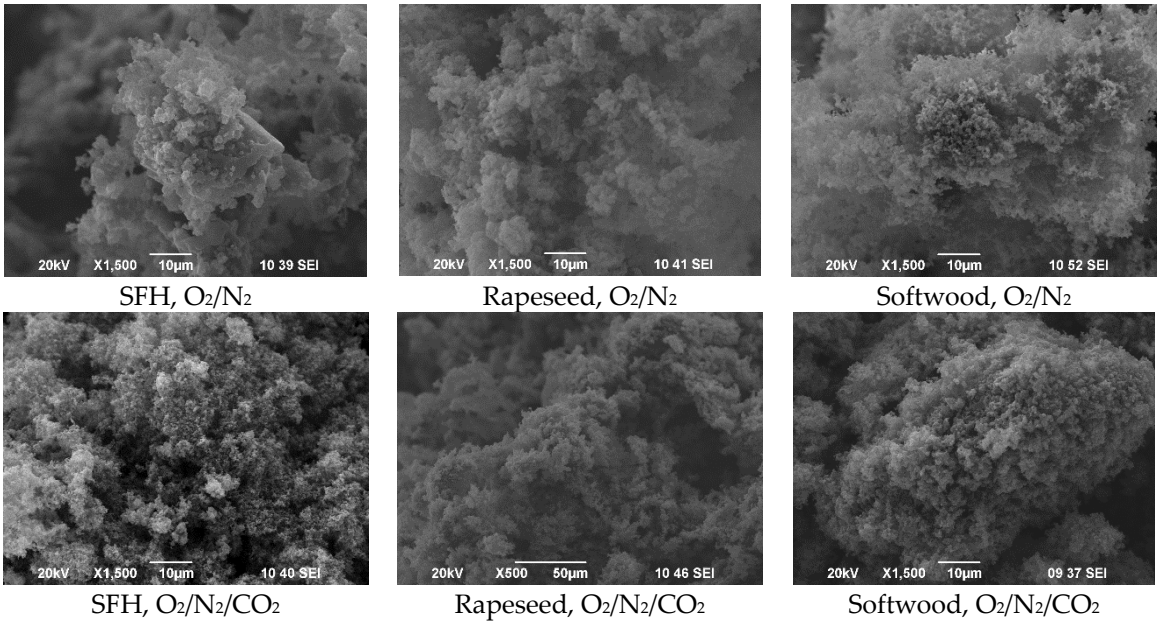

Figure 6. SEM images of PM from filter 8 (PM_1).

The volatile ash compounds, such as K and Cl, were found explicitly in all PM_1 collected during gasification of agricultural residue (rapeseed and sunflower husks) independently of the gasifying agent. This result is in line with the observations in [49]. The authors discussed that elements, like K and Cl, are incorporated in the fine particulates, through the processes of homogeneous vaporization, condensation, and nucleation.

Hermansson et al. [47] show PM chemical characterization, using handheld XRF analysis. The results showed that the elements K, S, and Cl are predominant in the submicron fractions of PM, while Ca, Si, and P are typically found in the supermicron particulates. These findings correspond well with the currently obtained EDS results.

Rapeseed is a traditional crop that gained significant interest during the last decades in the context of biofuel production. In the present experiment, this biomass showed the lowest PM emissions, even in presence of CO_2, in the gasification atmosphere. Thus, SEM/EDS analysis was carried out for the particles collected during rapeseed gasification with $O_2/N_2/CO_2$. In focus were the cyclone particles, as well as those, sampled in filters 5, 7, and 10 with the low-pressure impactor ($PM_{0.3}$, $PM_{0.65}$, and $PM_{2.5}$). The results are summarized in Table 3 and Figure 7a–d. Pictures (a) and (b) show the presence of dispersed large size particles, with a porous structure, varying geometrical shape and size. The images disclosed the existence of the char particles with a size larger than 100 µm.

Generally, the cyclone particulates and the PM in filter 10 ($PM_{2.5}$) showed heterogeneous structures according to their carbon content, C/O ratio, and mineral composition (Table 3, Figure 7a,b). These observations are in line with the work of [39,40,50]. The reported therein SEM results, concerning the top few filters (9–13), using a similar impactor, confirmed the presence of large char particles in the collected matter.

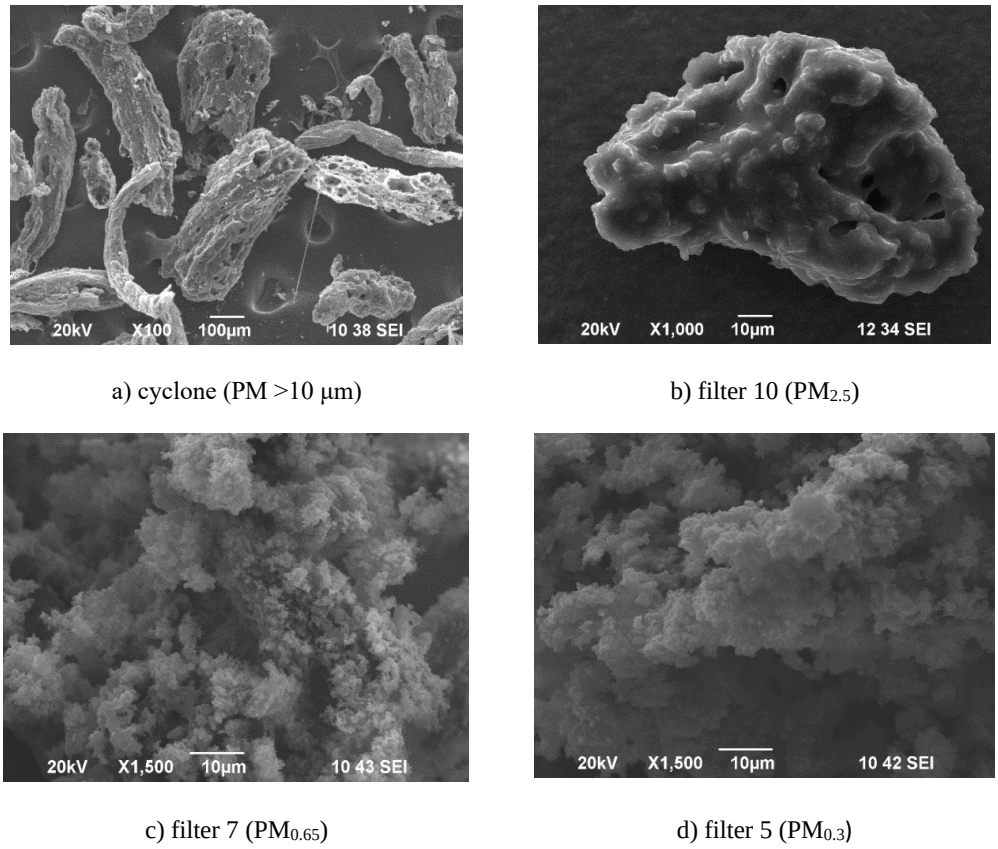

a) cyclone (PM >10 µm) b) filter 10 ($PM_{2.5}$)

c) filter 7 ($PM_{0.65}$) d) filter 5 ($PM_{0.3}$)

Figure 7. SEM images of rapeseed PM, sampled from different filters.

Table 3. Elemental composition of particulate matter, obtained through the EDS analysis.

Gasifying Gas	Biomass	PM	C	O	Cl	K	Mg	Ca	Cu	Na
			wt %							
O_2/N_2	SFH	PM_1	91.88 ± 0.79	6.45 ± 0.79	0.64 ± 0.09	1.03 ± 0.09				
	RP		88.08 ± 1.03	6.60 ± 1.03	2.43 ± 0.18	2.89 ± 0.19				
	SW		88.86 ± 1.40	11.14 ± 1.40						
$O_2/N_2/CO_2$	SFH		94.09 ± 1.50	5.09 ± 1.50	0.17 ± 0.11	0.65 ± 0.18				
	RP		90.23 ± 1.01	4.48 ± 1.00	1.92 ± 0.17	2.79 ± 0.19			0.59 ± 0.27	
	SW		94.63 ± 1.21	5.31 ± 1.21		0.06 ± 0.08				
$O_2/N_2/CO_2$	RP	(a) >10 µm	50.92 ± 1.99	28.23 ± 1.89		6.75 ± 0.39	0.81 ± 0.17	12.59 ± 0.63		0.7 ± 0.21
		(b) >10 µm	72.10 ± 1.58	18.30 ± 1.61		6.16 ± 0.34	0.17 ± 0.11	3.26 ± 0.27		
		(a) $PM_{2.5}$	58.37 ± 2.41	39.78 ± 2.38	0.25 ± 0.13	0.77 ± 0.18	0.32 ± 0.15	0.52 ± 0.26		
		(b) $PM_{2.5}$	90.54 ± 1.74	6.21 ± 1.75	0.56 ± 0.16	0.81 ± 0.18		1.89 ± 0.33		
		$PM_{0.65}$	89.68 ± 1.06	6.16 ± 1.07	1.70 ± 0.14	2.28 ± 0.16			0.18 ± 0.17	
		$PM_{0.3}$	87.97 ± 1.54	5.27 ± 1.55	2.93 ± 0.26	3.83 ± 0.3				

In the present experiment, the EDS of the rapeseed filters 5 and 7 ($PM_{0.3}$ and $PM_{0.65}$) showed carbon content of 87.97% ($PM_{0.3}$) and 89.68% ($PM_{0.65}$). Based on the SEM images (Figure 7c,d) and the EDS elemental composition (Table 3), it can be concluded that carbon (e.g., soot) was the dominating matter in these samples. The results correspond well with the work of [39,43,50]. All authors propose that the filters, consisting merely of soot particles, contain above 80% of carbon and represent submicron size PM.

Expectedly, all examined rapeseed particulates, except from both cyclones, showed the presence of Cl (0.13–0.26%) and K (0.18–0.34%). The cyclone particulates and those from filter 10 ($PM_{2.5}$) contained also Mg (0.11–0.15%) and Ca (0.26–0.33%) because alkaline earth metals are typical constituents of the bottom ash [49].

The appearance of Cu was found in some of the rapeseed filters (PM_1 and $PM_{0.65}$), whereas Na was found only in the cyclone particles.

A surface-sensitive quantitative spectroscopic technique (XPS) was used, thus supplementing the characterization of submicron size PM. The XPS analysis is still not a routine method in aerosol characterization, but it gains significant interest because the surface chemical composition has great potential to define the key optical parameters of aerosols with different origin and their specific reactivity [51].

Thus, the XPS analysis was applied to all filters 8, concerning the PM_1, obtained during a set of experiments with uncertainties of ±0.1 at %. The results are summarized in Table 4 and Figures 8 and 9.

Relatively low Al concentration was observed in the biomass ash analysis (Table 1) and this element was not detected by the EDS technique. The significant content of Al in the XPS spectra was associated mainly with the signal, originating from the filter's material [52]. Particulates from the filter that showed the maximum Al content, sunflower husks in $O_2/N_2/CO_2$, (see specter X11734), were placed on an Al-free conductive tape and an independent scan was shot, named X11735. This helped to differentiate the C-available in the lubricant placed on the Al filters (in the PM impactor), prior to the gasification experiment, as well as to demarcate the effects due to the intensive Al spectra.

The PM, captured on the Al filters was analyzed at a depth up to 5 nm, whereas the chemical composition specimen, placed on the conductive tape was obtained for the entire sample volume. The chemical composition of PM_1 was estimated from the total scan of each filter/specimen.

Comparing the composition in X11734 and X11735 the carbon content in X11735 was higher. Noticeable was the fact that the entire tape's surface was covered with PM, whereas the particulates on the Al-filter's surface (X11734) were unevenly distributed. The effect was observable also when the elements Al and O were compared (Table 4). The elevated concentration of both elements, according to the X11734 spectra, was attributed to the availability of Al^{3+}. Detailed spectra of Al2p (not presented), revealed that the surface of the alumina filters was covered with $Al(OH)_3$ and AlOOH [52].

The chemical composition obtained with the XPS technique corresponded well with the EDS analysis, confirming that the primary PM_1 component was carbon, due to the incomplete oxidation. The effect of the gasifying agent was also clearly observable, resulting in elevated carbon in the presence of CO_2. The elements O and Si were obtained in all PM_1 specimens, along with the low concentration of Cl, and Ca in some of the filters.

Table 4. Chemical composition of PM1 obtained through XPS analysis.

Gasifying Agent	Biomass	Specter Name	C	O	Al	Si	Ca	Cl
			at %					
O_2/N_2	SFH	X11739	89.0	5.9	4.1	0.6		0.4
	Rapeseed	X11736	89.5	4.9	4.0	0.9		0.7
	Softwood	X11737	82.5	8.3	8.7	0.6		
$O_2/CO_2/N_2$	SFH	X11734	74.0	12.9	11.9	0.4	0.4	0.5
	SFH (Al-free)	X11735	95.7	3.0	0.0	1.2		0.1
	Rapeseed	X11740	92.9	3.7	2.1	0.8		0.5
	Softwood	X11738	96.1	2.2	1.3	0.4		

Deconvolution of the C1s; O1s; Si2p; Cl2p spectra helped to identify the chemical state of the elements. Detailed analysis of the C1s spectra showed the general oxygen-containing groups. An example is shown in Figure 9 for the deconvolution of the X11735 (C1s)

spectra (Figure 9, left), obtained for the PM_1 from sunflower husk on the conductive tape, which showed three peaks at BE of 285.3; 286.3, and 287.1 eV. According to [53–57], the peak at 285.3 eV was related to the existence of poorly oxidized carbon chains (e.g., –CH–CH–; –C–O). The one at 286.3 eV was attributed to carbon involved in –C–O–C– bonds (including aromatic structures), as well as in C–OH, whereas the peak at 287.1 eV was associated with carbonyl groups (–C=O).

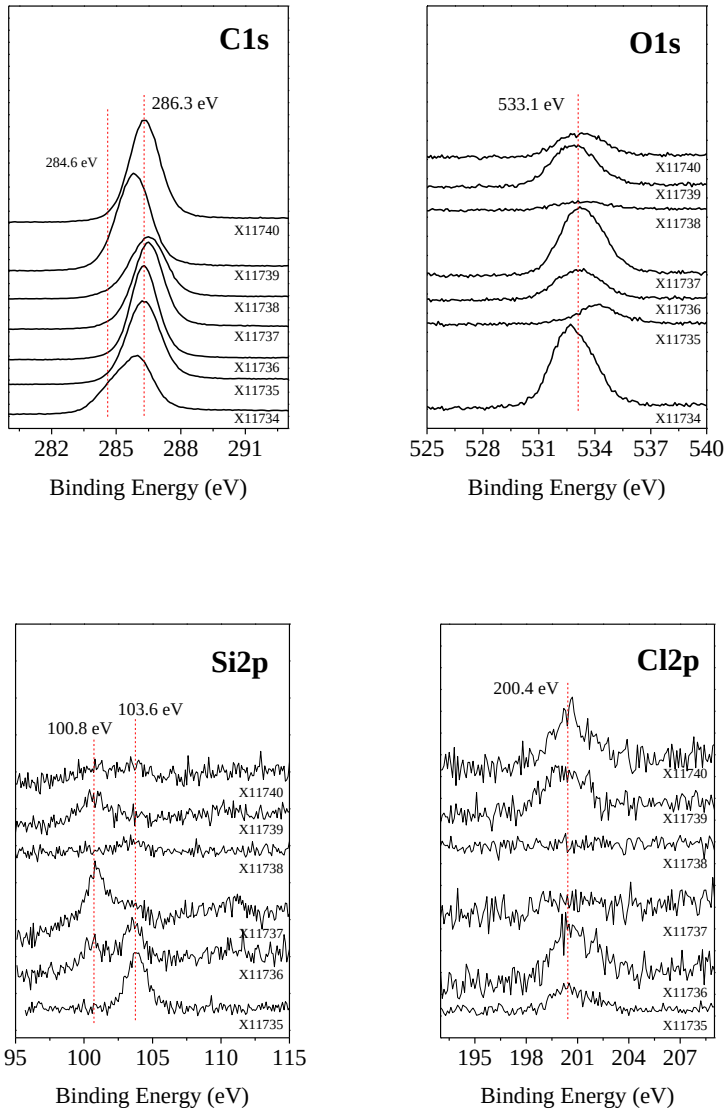

Figure 8. XPS spectra of PM_1 for three biomass types and two gasifying agents (O_2/N_2 and $O_2/N_2/CO_2$).

The C1s spectra (X11734—Figure 9, right) showed three peaks at 284.8, 286.0, and 287.6 eV. The first peak was associated solely with –C–C– bonds, which were not observed in X11735 (C1s), the specimen on the conductive tape. It allowed us to conclude that the first peak in X11734 was due to the lubricant on the alumina filter. The next two peaks (286.0 and 287.6 eV in X11734) referred to carbon involved in –C–O–C– and –C=O bonds.

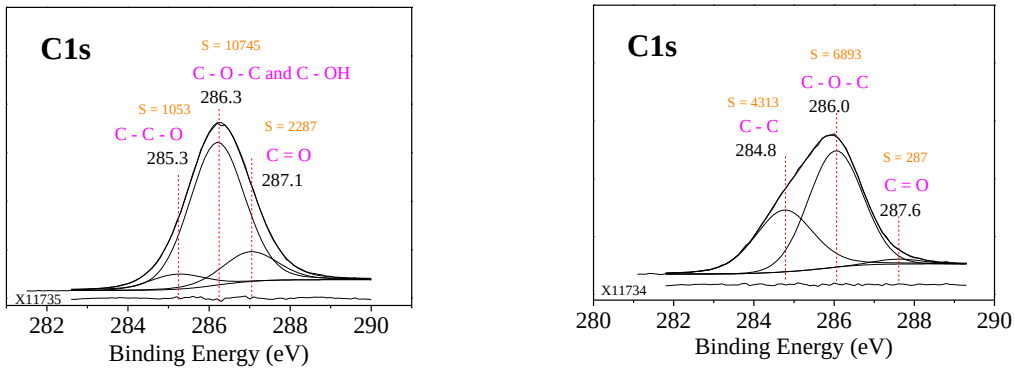

Figure 9. Chemical-state analysis of carbon (C1s) from the XPS spectra of PM_1, derived from sunflower husk gasification in $O_2/N_2/CO_2$.

The spectra of Si_2p (not present) revealed two phases: one at 103.6 eV, corresponding to SiO_2, and another at 100.8 eV, showing the existence of organically bound Si 48–50. The BE of the peaks of Cl_2p at 200.4 eV (also not present) confirmed that the Cl in PM_1, was involved in hydrocarbon chains.

The present XPS results are in line with the XPS spectra of atmospheric PM of different sizes, reported in [51,58]. The detailed analysis of C1s in [51] showed that the main oxygen-containing groups were: carbonylic, carboxylic, and carbonate groups. The results in [58] from the high- resolution XPS spectra of atmospheric PM suggested the following organic functional groups (C–C/C=C, –C–O, C–O/–C(O)N, –C(O)O, CO_3=), as well were involved inorganic elements like sulfur (SO_4^{2}+, sulphone, and sulfide compounds); nitrogen (NH_4^+, NO_3^-, NO_2^- and organic-N compounds); sodium (Na^+) and chlorine (Cl^-).

4. Conclusions

The present work was focused on biomass (rapeseed, softwood, and sunflower husks) gasification in a DTF. The experiments were carried out using two different gasifying agents (O_2/N_2 and $O_2/N_2/CO_2$) at atmospheric pressure and a constant temperature of 1000 °C. The effect of biomass and gasifying agent on the following parameters was investigated: syngas composition (CO, H_2, CH_4, and CO_2); CGE and CCE; emissions of cyclone particles and PM emissions and their chemical characterization using SEM/EDS and XPS techniques. The main conclusions were as follows:

- The introduction of CO_2 increased the production of CO and CH_4, while there was a decrease in CO_2 and H_2. The syngas LHV was also slightly higher. These results enhanced the CGE and CCE.
- Because CO_2 decreased the production of H_2, it resulted in a lower H_2/CO ratio. Rapeseed had the highest H_2/CO ratio and the highest carbon conversion efficiency, while softwood had the highest cold gas efficiency. Most of the generated syngas can be used for the synthesis of higher hydrocarbons since the H_2/CO ratio was between 0.25 and 0.9.
- Another effect of CO_2 containing gasifying atmosphere was the lowered emissions of cyclone particles, while the total mass of the $PM_{10–0.03}$ has increased regardless of the biomass type. Particulates of submicron size were the dominant fraction ($PM_{1–0.3}$) in O_2/N_2 and $PM_{1.6–0.3}$ in $O_2/N_2/CO_2$. Unimodal PM size distribution was observed, except for sunflower husks gasification in $O_2/N_2/CO_2$, for which bimodal PM distribution was determined. All PM peaks in the CO_2 atmosphere were slightly shifted to the right, but still in the submicron range of PM size. The effect of CO_2 concentration (in the gasifying atmosphere) and the temperature was not subject to the present work. However, further optimization experiments are required,

aiming to reduce the overall PM yield while keeping the process efficiency or even improving it.

- The SEM/EDS and the XPS results confirmed that submicron-sized PM contains above 80% of carbon, which is considered to be mainly soot, formed due to the incomplete biomass oxidation. The carbon content gradually decreased in the larger particulates, reaching about 50% in cyclone (char) particles, on the account of the ash mineral composition. The SEM/EDS results confirmed that alkali metals, such as K and Cl were typical constituents of the submicron size PM, whereas the alkaline earth metals were found in the fine and coarse particles. Detailed analysis of the XPS (C1s, O1s, Si_2p, and Cl_2p) spectra allowed determining the most common oxygen-containing carbon groups on the PM_1 surface (carbonyl and carboxyl), along with the appearance of –C–OH, –CH–CH, and aryl groups, as well as inorganic and organically bound mineral compounds (e.g., SiO_2, organically bound Si and Cl).

Author Contributions: R.F.: experimental work, results analysis and visualization, writing and editing original draft, corresponding author. T.P.: experimental work, results analysis, data validation and visualization, writing and editing original draft. A.F.F.: results analysis and visualization, writing and editing original draft. M.C.: conceptualization, methodology, supervision. I.I.: conceptualization, methodology, data validation and visualization, writing and editing original draft, supervision. S.A.-V.: SEM/EDS analysis and data processing, B.R.: SEM/EDS analysis and data processing. All authors have read and agreed to the published version of the manuscript.

Funding: This research was partially supported by the Fundação para a Ciência e a Tecnologia (FCT) through IDMEC, under LAETA, project UID/EMS/50022/2019, project UIDB/50022/2020 and project PTCD/EME-EME/30300/2017. The authors Iliyana Inaydenova and Tsvetelina Petrova would like to acknowledge the financial support from the National Science Program "Environmental Protection and Reduction of Risks of Adverse Events and Natural Disasters", approved by the Resolution of the Council of Ministers No 577/17.08.2018 and supported by the Ministry of Education and Science of Bulgaria (Agreement No D01-230/06.12.2018 and Agreement No Д01-322/18.12.2019). Bogdan Ranguelov acknowledges the support from Project INFRAMAT D01–284/17.12.2019 with Ministry of Education and Science, Bulgaria.

Institutional Review Board Statement: Not applicable.

Informed Consent Statement: Not applicable.

Data Availability Statement: Not applicable.

Acknowledgments: The authors would like to express their deep hearty gratitude Mário Costa for sharing his knowledge and field experience, work, support, motivation, opportunities, legacy and mark that he left to everyone who had the privilege of working with him. It was a pleasure working with you, Mário Costa. Rest in peace!

Conflicts of Interest: The authors declare no conflict of interest.

References

1. Popp, J.; Lakner, Z.; Harangi-Rákos, M.; Fári, M. The effect of bioenergy expansion: Food, energy, and environment. *Renew. Sustain. Energy Rev.* **2014**, *32*, 559–578, doi:10.1016/j.rser.2014.01.056.
2. Koleva, E.G.; Mladenov, G.M. Renewable Energy and Energy Efficiency in Bulgaria. *Prog. Ind. Ecol.* **2014**, *8*, 257–278, doi:10.1504/PIE.2014.066798.
3. Zhang, Y.; Kajitani, S.; Ashizawa, M.; Oki, Y. Tar Destruction and Coke Formation during Rapid Pyrolysis and Gasification of Biomass in a Drop-Tube Furnace. *Fuel* **2010**, *89*, 302–309, doi:10.1016/j.fuel.2009.08.045.
4. Zhai, M.; Zhang, Y.; Dong, P.; Liu, P. Characteristics of Rice Husk Char Gasification with Steam. *Fuel* **2015**, *158*, 42–49, doi:10.1016/j.fuel.2015.05.019.
5. Stevens, D.J. *Hot Gas Conditioning: Recent Progress with Larger-Scale Biomass Gasification Systems*; National Renewable Energy Lab.: Golden, CO, USA, 2001; doi:10.2172/786288.
6. Stoilov, S.; Marinov, K.I.; Gochev, Z. Biomass Potential of Bulgarian Forest-Based Sector for Energy Production. In Proceedings of the 6th International Science Conference "Chip and Chipless Woodworking Processes", Šturovo, Slovakia, 11–13 September 2008.

7. Bell, D.; Towler, B.; Fan, M. *Coal Gasification and Its Applications*; Elsevier Inc. 2010; doi:10.1016/C2009-0-20067-5. Available online: https://www.sciencedirect.com/book/9780815520498/coal-gasification-and-its-applications?via=ihub=#book-info (accessed on 8 January 2021).
8. Higman, C.; Tam, S. Advances in Coal Gasification, Hydrogenation, and Gas Treating for the Production of Chemicals and Fuels. *Chem. Rev.* **2014**, *114*, 1673–1708, doi:10.1021/cr400202m.
9. La Villetta, M.; Costa, M.; Massarotti, N. Modelling Approaches to Biomass Gasification: A Review with Emphasis on the Stoichiometric Method. *Renew. Sustain. Energy Rev.* **2017**, *74*, 71–88, doi:10.1016/j.rser.2017.02.027.
10. Agarwal, R.; Awasthi, A.; Singh, N.; Mittal, S.K.; Gupta, P.K. Epidemiological Study on Healthy Subjects Affected by Agriculture Crop-Residue Burning Episodes and Its Relation with Their Pulmonary Function Tests. *Int. J. Environ. Health Res.* **2013**, *23*, 281–295, doi:10.1080/09603123.2012.733933.
11. Asadullah, M. Biomass Gasification Gas Cleaning for Downstream Applications: A Comparative Critical Review. *Renew. Sustain. Energy Rev.* **2014**, *40*, 118–132, doi:10.1016/j.rser.2014.07.132.
12. Bond, T.C.; Doherty, S.J.; Fahey, D.W.; Forster, P.M.; Berntsen, T.; Deangelo, B.J.; Flanner, M.G.; Ghan, S.; Kärcher, B.; Koch, D.; et al. Bounding the Role of Black Carbon in the Climate System: A Scientific Assessment. *J. Geophys. Res. Atmos.* **2013**, *118*, 5380–5552, doi:10.1002/jgrd.50171.
13. Billaud, J.; Valin, S.; Peyrot, M.; Salvador, S. Influence of H_2O, CO_2 and O_2 Addition on Biomass Gasification in Entrained Flow Reactor Conditions: Experiments and Modelling. *Fuel* **2016**, *166*, 166–178, doi:10.1016/j.fuel.2015.10.046.
14. Qin, K.; Jensen, P.A.; Lin, W.; Jensen, A.D. Biomass Gasification Behavior in an Entrained Flow Reactor: Gas Product Distribution and Soot Formation. *Energy Fuels* **2012**, *26*, 5992–6002, doi:10.1021/ef300960x.
15. Qin, K.; Lin, W.; Jensen, P.A.; Jensen, A.D. High-Temperature Entrained Flow Gasification of Biomass. *Fuel* **2012**, *93*, 589–600, doi:10.1016/j.fuel.2011.10.063.
16. Pohořelý, M.; Jeremiáš, M.; Svoboda, K.; Kameníková, P.; Skoblia, S.; Beňo, Z. CO_2 as Moderator for Biomass Gasification. *Fuel* **2014**, *117*, 198–205, doi:10.1016/j.fuel.2013.09.068.
17. Gao, Y.; Wang, X.; Chen, Y.; Li, P.; Liu, H.; Chen, H. Pyrolysis of Rapeseed Stalk: Influence of Temperature on Product Characteristics and Economic Costs. *Energy* **2017**, *122*, 482–491, doi:10.1016/j.energy.2017.01.103.
18. Burhenne, L.; Messmer, J.; Aicher, T.; Laborie, M.P. The Effect of the Biomass Components Lignin, Cellulose and Hemicellulose on TGA and Fixed Bed Pyrolysis. *J. Anal. Appl. Pyrolysis* **2013**, *101*, 177–184, doi:10.1016/j.jaap.2013.01.012.
19. Sattar, A.; Leeke, G.A.; Hornung, A.; Wood, J. Steam Gasification of Rapeseed, Wood, Sewage Sludge and Miscanthus Biochars for the Production of a Hydrogen-Rich Syngas. *Biomass Bioenergy* **2014**, *69*, 276–286, doi:10.1016/j.biombioe.2014.07.025.
20. Mandl, C.; Obernberger, I.; Scharler, I.R. Characterisation of Fuel Bound Nitrogen in the Gasification Process and the Staged Combustion of Producer Gas from the Updraft Gasification of Softwood Pellets. *Biomass Bioenergy* **2011**, *35*, 4595–4604, doi:10.1016/j.biombioe.2011.09.001.
21. Aghaalikhani, A.; Schmid, J.C.; Borello, D.; Fuchs, J.; Benedikt, F.; Hofbauer, H.; Rispoli, F.; Henriksen, U.B.; Sárossy, Z.; Cedola, L. Detailed Modelling of Biomass Steam Gasification in a Dual Fluidized Bed Gasifier with Temperature Variation. *Renew. Energy* **2019**, *143*, 703–718, doi:10.1016/j.renene.2019.05.022.
22. Tsalidis, G.A.; Di Marcello, M.; Spinelli, G.; de Jong, W.; Kiel, J.H.A. The Effect of Torrefaction on the Process Performance of Oxygen-Steam Blown CFB Gasification of Hardwood and Softwood. *Biomass Bioenergy* **2017**, *106*, 155–165, doi:10.1016/j.biombioe.2017.09.001.
23. Mauerhofer, A.M.; Fuchs, J.; Müller, S.; Benedikt, F.; Schmid, J.C.; Hofbauer, H. CO_2 Gasification in a Dual Fluidized Bed Reactor System: Impact on the Product Gas Composition. *Fuel* **2019**, *253*, 1605–1616, doi:10.1016/j.fuel.2019.04.168.
24. Bulgarian Ministry of Agriculture, Food and Forestry. Available online: https://www.mzh.government.bg/en/ (accessed on 8 January 2021).
25. Cabuk, B.; Duman, G.; Yanik, J.; Olgun, H. Effect of Fuel Blend Composition on Hydrogen Yield in Co-Gasification of Coal and Non-Woody Biomass. *Int. J. Hydrogen Energy* **2020**, *45*, 3435–3443, doi:10.1016/j.ijhydene.2019.02.130.
26. Behainne, J.J.R.; Martinez, J.D. Performance Analysis of an Air-Blown Pilot Fluidized Bed Gasifier for Rice Husk. *Energy Sustain. Dev.* **2014**, *18*, 75–82, doi:10.1016/j.esd.2013.11.008.
27. Mojaver, P.; Jafarmadar, S.; Khalilarya, S.; Chitsaz, A. Study of Synthesis Gas Composition, Exergy Assessment, and Multi-Criteria Decision-Making Analysis of Fluidized Bed Gasifier. *Int. J. Hydrogen Energy* **2019**, *44*, 27726–27740, doi:10.1016/j.ijhydene.2019.08.240.
28. Chuturkova, R. Particulate matter air pollution (PM_{10} and $PM_{2.5}$) in urban and industrial areas. *J. Sci. Educ. Innov.* **2015**, *5*, 13–32.
29. Dimitrova, M.; Trenchev, P.; Georgieva, E.; Neykova, N.; Neykova, R.; Nedkov, R.; Gochev, D.; Syrakov, D.; Veleva, B.; Atanassov, D.; et al. Seasonal changes of aerosol pollutants over Bulgaria. In Proceedings of the 15th International Scientific Conference SES 2019, Sofia, Bulgaria, 6–8 November 2019; pp. 241–252.
30. Naydenova, I.; Petrova, T.; Velichkova, R.; Simova, I. PM_{10} Exceedance In Bulgaria. In Proceedings of the CBU International Conference on Innovations in Science and Education 2018, Prague, Czech Republic, 21–23 March 2018.
31. Neykova, R.; Hristova, E. Application of Backward Trajectories and Cluster Analyses for Study of Variations in PM_{10} Concentrations. In Proceeding of the 1st International Conference on Environmental Protection and Disaster RISKs, Sofia, Bulgaria, 29–30 September 2020; pp. 170–179, doi:10.48365/ENVR-2020.1.15.
32. Veleva, B.; Hristova, E.; Nikolova, E.; Kolarova, M.; Valcheva, R. Seasonal variation of PM_{10} elemental composition in urban environment. *J. Int. Sci. Publ. Ecol. Saf.* **2014**, *8*, 265–275.

33. Veleva, B.; Hristova, E.; Nikolova, E.; Kolarova, M.; Valcheva, R. Elemental composition of air particulate (PM_{10}) in Sofia by EDXRF techniques. *J. Chem. Technol. Metall.* **2014**, *49*, 163–169.
34. Veleva, B.; Hristova, E.; Nikolova, E.; Kolarova, M.; Valcheva, R. Experimental study on elemental composition of PM_{10} in Sofia, 2012–2014. *Sci. Technol.* 2015, *V*, doi:10.13140/RG.2.1.4570.8562.
35. Nikolaev, A.; Konidari, P. Development and Assessment of Renewable Energy Policy Scenarios by 2030 for Bulgaria. *Renew. Energy* **2017**, *111*, 792–802, doi:10.1016/j.renene.2017.05.007.
36. Energy, N.; Action, E. Republic of Bulgaria Ministry of Economy and Energy. 2014, 2019, 1–93. Available online: https://www.seea.government.bg/documents/2014_neeap_en_bulgaria.pdf (accessed on 8 January 2021).
37. Executive Environment Agency at the Ministry of Environment and Water. *Bulgaria's Informative Inventory Report 2019 (IIR)*; Submission under the UNECE Convention on Long-Range Transboundary Air Pollution, Centre on Emission Inventories and Projections (CEIP); Umweltbundesamt: Vienna, Austria, 2019.
38. Naydenova, I.; Sandov, O.; Wesenauer, F.; Laminger, T.; Winter, F. Pollutants Formation during Single Particle Combustion of Biomass under Fluidized Bed Conditions: An Experimental Study. *Fuel* **2020**, *278*, 117958, doi:10.1016/j.fuel.2020.117958.
39. F.S Duarte. Biomass Gasification in a Drop Tube Furnace. Master's Thesis, IST, Lisboa, Portugal, 2018.
40. Duarte, F.; Ferreiro, A.I.; Costa, M. Soot Formation during the Gasification of Wheat Straw in a Drop Tube Furnace. In Proceedings of the 5th International Conference WASTES: Solutions, Treatments and Opportunities, Costa da Caparica, Portugal, 4–6 September 2019.
41. Shen, Y.; Li, X.; Yao, Z.; Cui, X.; Wang, C.H. CO_2 Gasification of Woody Biomass: Experimental Study from a Lab-Scale Reactor to a Small-Scale Autothermal Gasifier. *Energy* **2019**, *170*, 497–506, doi:10.1016/j.energy.2018.12.176.
42. Waldheim, L.; Nilsson, T. Heating Value of Gases from Biomass Gasification. Report for IEA Bioenergy Agreement, Task. 20—Therm. Gasif. Biomass 2001, No. May, 61. Available online: http://www.ieatask33.org/download.php?file=files/file/publications/HeatingValue.pdf (accessed on 8 January 2021).
43. Adánez-Rubio, I.; Ferreira, R.; Rio, T.; Alzueta, M.U.; Costa, M. Soot and Char Formation in the Gasification of Pig Manure in a Drop Tube Reactor. *Fuel* **2020**, *281*, 118738, doi:10.1016/j.fuel.2020.118738.
44. Saad, J.M.; Williams, P.T. Manipulating the H_2/CO Ratio from Dry Reforming of Simulated Mixed Waste Plastics by the Addition of Steam. *Fuel Process. Technol.* **2017**, *156*, 331–338, doi:10.1016/j.fuproc.2016.09.016.
45. Nyström, R. Particle Emissions from Residential Wood and Biodiesel Combustion. Ph.D. Thesis, Umeå University, Umeå, Sweden, 2016.
46. Gao, X.; Wu, H. Combustion of Volatiles Produced in Situ from the Fast Pyrolysis of Woody Biomass: Direct Evidence on Its Substantial Contribution to Submicrometer Particle (PM1) Emission. *Energy Fuels* **2011**, *25*, 4172–4181, doi:10.1021/ef2008216.
47. Hermansson, S.; Hjörnhede, A.; Seemann, M. *Particulate Matter in the Product Gas from Indirect Biomass Gasification (Partikulära Föroreningar i Produktgasen Från Indirekt)*; Report of Swedish Gas Technology Centre; Swedish Gas Technology Centre: Malmö, Sweden, 2013. Available online: http://www.sgc.se/ckfinder/userfiles/files/SGC275.pdf (accessed on 8 January 2021).
48. Chen, H.; Tang, X.; Liang, C.; Wu, X. Attapulgite Suspension Mitigates Fine Particulate Matter (PM2.5) Emission from Coal Combustion in Fluidized Bed. *J. Environ. Manag.* **2018**, *209*, 245–253, doi:10.1016/j.jenvman.2017.12.072.
49. Obernberger, I.; Brunner, T.; Bärnthaler, G. Chemical Properties of Solid Biofuels—Significance and Impact. *Biomass Bioenergy* **2006**, *30*, 973–982, doi.org/10.1016/j.biombioe.2006.06.011.
50. Kurian, V. Asphaltene Gasification: Soot Formation and Metal Distribution. Ph.D. Thesis. University of Alberta, Edmonton, AB, Canada, 2016; p. 160.
51. Guascito, M.; Ielpo, P.; Cesari, D.; Genga, A.; Malitesta, C.; Picca, R.; Contini, D.C. Application of Xps Surface Analysis for Characterizationof Size-Segregated Particulate Matter from a Urban Background Site in Lecce. In Proceedings of the Symposium on Environmental Instrumentation and Measurements Protecting Environment, Climate Changes and Pollution Control, Lecce, Italy, 3–4 June 2013.
52. Wagner, C.D.; Passoja, D.E.; Hillery, H.F.; Kinisky, T.G.; Six, H.A.; Jansen, W.T.; Taylor, J.A. Auger and Photoelectron Line Energy Relationships in Al-O and Si-O Compounds. *J. Vac. Sci. Technol.* **1982**, *21*, 933–944.
53. Beamson, G.; Briggs, D. High Resolution XPS of Organic Polymers. *J. Chem. Educ.* **1993**, doi.org/10.1021/ed070pA25.5.
54. Permatasari, F.A.; Aimon, A.H.; Iskandar, F.; Ogi, T.; Okuyama, K. Role of C-N Configurations in the Photoluminescence of Graphene Quantum Dots Synthesized by a Hydrothermal Route. *Sci. Rep.* **2016**, *6*, 21042, doi:10.1038/srep21042.
55. Mattevi, C.; Eda, G.; Agnoli, S.; Miller, S.; Mkhoyan, K.A.; Celik, O.; Mastrogiovanni, D.; Granozzi, G.; Carfunkel, E.; Chhowalla, M. Evolution of Electrical, Chemical, and Structural Properties of Transparent and Conducting Chemically Derived Graphene Thin Films. *Adv. Funct. Mater.* **2009**, *19*, 2577–2583, doi:10.1002/adfm.200900166.
56. Gonzalez-Elipe, A.R.; Espinos, J.P.; Munuera, G.; Sanz, J.; Serratosa, J.M.; Bonding-state characterization of constituent elements in phyllosilicate minerals by XPS and NMR. *J. Phys. Chem.* **1988**, *92*, 3471–3476, doi:10.1021/j100323a031.
57. Naumkin, A.V.; Kraut-Vass, A.; Gaarenstroom, S.W.; Powell, C.J. NIST Standard Reference Database 20, V. 4.1 (Web Version). 2012. Available online: http:/srdata.nist.gov/xps/ (accessed on 8 January 2021).
58. Guascito, M.R.; Cesari, D.; Chirizzi, D.; Genga, A.; Contini, D. XPS Surface Chemical Characterization of Atmospheric Particles of Different Sizes. *Atmos. Environ.* **2015**, *116*, 146–154, doi:10.1016/j.atmosenv.2015.06.028.